Multi-region Control for Urban Road Networks Using Adaptive Optimization

Anastasios Kouvelas
Mohammadreza Saeedmanesh
Nikolas Geroliminis

École Polytechnique Fédérale de Lausanne

April 2015

STRC

15th Swiss Transport Research Conference

Monte Verità / Ascona, April 15 – 17, 2015

École Polytechnique Fédérale de Lausanne

Multi-region Control for Urban Road Networks Using Adaptive Optimization

Anastasios Kouvelas, Mohammadreza Saeedmanesh
Urban Transport Systems Laboratory
École Polytechnique Fédérale de Lausanne
GC C2 390, Station 18, 1015 Lausanne
phone: +41-21-69-35397
fax: +41-21-69-35060
{tasos.kouvelas,mohammadreza.saeedmanesh}@epfl.ch

Nikolas Geroliminis
Urban Transport Systems Laboratory
École Polytechnique Fédérale de Lausanne
GC C2 389, Station 18, 1015 Lausanne
phone: +41-21-69-32481
fax: +41-21-69-35060
nikolas.geroliminis@epfl.ch

April 2015

Abstract

In this paper we present a control scheme for heterogeneous transportation networks which is based on the concept of the Macroscopic Fundamental Diagram (MFD) integrated with an adaptive optimization technique. The heterogeneous transportation network is first partitioned into a number of regions with homogeneous traffic conditions and well-defined MFDs. An appropriate clustering algorithm that consumes traffic information is applied for that purpose. A macroscopic MFD-based model is used to describe the traffic dynamics of the resulting multi-region transportation system. A multivariable proportional integral (PI) feedback regulator is implemented to control the nonlinear system in real-time. The control variables consist of the inter-transferring flows between neighbourhood regions and the actuators correspond to the traffic lights of these areas (e.g. boundaries between regions). The recently proposed Adaptive Fine-Tuning (AFT) algorithm is used to optimize the gain matrices as well as the vector with the set-points of the PI controller. AFT is an iterative adaptive algorithm that optimizes the values of the tuneable parameters of the controller (e.g. gains and set-points) based on measurements of a performance index (e.g. total delay) for different perturbations of the parameters. In each iteration AFT receives (a) the total delay of the system and (b) some aggregate information about the demand of each region and calculates the control parameters to be used at the next iteration. The overall control scheme is tested in simulation and different performance criteria are studied. The performance of the initial PI controller which corresponds to a fixed-time policy is compared to the final controller that is obtained after the convergence of AFT. A key advantage of the proposed approach is that it does not require high computational effort and future demand data if the current state of each region can be observed with loop detector data.

Keywords

Macroscopic fundamental diagram; adaptive optimization; urban signal control

1 Introduction

Traffic congestion is a major problem of urban environments and modern metropolitan areas. Real-time traffic management is deemed to be an efficient and cost effective way to ameliorate traffic conditions and prevent gridlock phenomena in cities. Although many methodologies have been developed for real-time signal control over the last decades (see e.g. Papageorgiou *et al.* (2003) for a good review), the design of efficient control strategies for heterogeneous large-scale urban networks that can deal with oversaturated conditions (where queues spill back to upstream links) remains a significant challenge. Strategies that are widely used around the world like SCOOT (Hunt *et al.,* 1982) and SCATS (Lowrie, 1982) are based on heuristic optimization techniques and are not efficient when the network faces propagation phenomena. Other traffic responsive strategies (Gartner, 1983, Farges *et al.,* 1983, Mirchandani and Head, 1998) use complex optimization methods which make their online application to large-scale urban networks difficult due to high computational requirements. TUC (Diakaki *et al.,* 2002, 2003) and its recent extensions (Aboudolas *et al.,* 2010, Kouvelas *et al.,* 2011b) is a practicable network-wide control strategy which applies a multivariable feedback regulator approach that derives from a Linear-Quadratic optimal control problem. TUC tries to deal with oversaturated conditions by minimizing and balancing the relative occupancies of the network links. However, in the case of heterogeneous networks with multiple pockets of congestion and heavily directional demand flows this type of control may not be optimal.

An alternative approach for real-time network-wide control for heterogeneous urban networks that has recently gain a lot of interest is the perimeter control (or gating). The basic concept of such an approach is to partition the heterogeneous network into a small number of homogeneous regions and apply perimeter control to the inter-transferring flows along the boundaries of each region. The input flows to a region (which are also output flows for the neighbouring regions) can be controlled at the intersections located at the borders of the region, so as to maximize the total throughput of the system. Perimeter control (or gating) policies have been introduced for single-region homogeneous networks (Daganzo, 2007, Keyvan-Ekbatani *et al.,* 2012) and multi-region heterogeneous networks (Haddad and Geroliminis, 2012, Geroliminis *et al.,* 2013, Aboudolas and Geroliminis, 2013) using different control methodologies.

The key modelling tool that is used by all the aforementioned strategies is the Macroscopic Fundamental Diagram (MFD), which provides a concave, low-scatter relationship between network vehicle accumulations (veh) or density (veh/km) and network circulating flow (veh/h). The concept of a network MFD was firstly introduced in Godfrey (1969), but the empirical verification of its existence with dynamic features is recent (Geroliminis and Daganzo, 2008). Given also that a stable linear relation exists between circulating (or space-mean) flow and region

outflow (vehicles finishing their trips) due to time-invariant regional trip length (Geroliminis and Daganzo, 2008), MFD can be also expressed as outflow (trip completion rate) versus accumulation. Estimating the circulating flow of a region is much easier as it is directly measured by loop detectors, whereas outflow would require installation of detectors at the borders of each region or very high penetration rate of GPS data.

The existence of low-scatter MFD and the stability of its shape under different O-D patterns and adaptive control remain a research question. The main challenges are hysteresis phenomena that appear at the onset or offset of congestion and the heterogeneity of traffic in urban networks. Heterogeneous networks do not have a well-defined MFD, especially in the congested regime. Partitioning such a network into homogeneous regions (i.e. areas with compact shape that have small variance of link densities) can result in well-defined MFD as shown in (Ji and Geroliminis, 2012). The objectives of partitioning are to obtain (i) small variance of link densities within a region, which increases the network flow for the same average density and (ii) spatial compactness of each region which makes feasible the application of perimeter transferring flow control. The MFD concept has already been used for designing control policies, as it provides aggregated relationships between traffic variables and reduces the complexity of traffic flow dynamics for model-based approaches (e.g. model predictive control).

There are only few works (Geroliminis *et al.,* 2013, Aboudolas and Geroliminis, 2013) that deal with perimeter control for multi-region systems with MFD-based modelling. However, none of this works deals with parameter uncertainties in the model or short-term and long-term variations in the dynamics of the system. In Geroliminis *et al.* (2013) a model predictive control approach is proposed and a nonlinear MFD-based model is used to describe the dynamics of the system. Although the controller is tested for different levels of error in the MFDs and the demand profiles, perfect information about the model parameters is assumed. In Aboudolas and Geroliminis (2013) a Linear-Quadratic state feedback Regulator (LQR) and two versions of the optimization problem (with and without integral action) are studied. The LQ/LQI gain matrices are designed by linearizing the nominal nonlinear traffic dynamics around the equilibrium points. Note that such nominal-optimal control laws do no guarantee the robustness properties with respect to uncertainties. Some more recent works (Haddad and Mirkin, 2015, Ampountolas and Kouvelas, 2015) try to deal with adaptive schemes in order to improve the performance of the controller.

In this work a multivariable proportional integral (PI) feedback regulator is implemented to control the multi-region system. The structure of the PI controller is similar to the ones used in Keyvan-Ekbatani *et al.* (2012) and Aboudolas and Geroliminis (2013), however the gain matrices and the targets (set-points) of the controller are updated in real-time based on performance measurements by an adaptive optimization algorithm. The overall control scheme is tested

in microsimulation for the urban network of Barcelona, Spain and the impact of the applied perimeter control is evaluated via the corresponding MFDs and other performance measures. More precisely, the derived control scheme (which only affects a small number of intersections at the boundaries between regions) is compared to the case where fixed-time control is applied to the network.

2 Aggregated dynamics for multi-region system based on MFDs

Consider an urban network partitioned in N homogeneous regions with well-defined MFDs (see Figure 1). The index $i \in \mathcal{N} = \{1, 2, \ldots, N\}$ denotes the region of the system, $n_i(t)$ the total accumulation (number of vehicles) in region i and $n_{ij}(t)$ the number of vehicles in region i with final destination region $j \in \mathcal{N}$, at a given time t. Let $\mathcal{N}_i$ be the set of all regions that are directly reachable from the borders of region i, i.e. adjacent regions to region i. The discrete time dynamics of the N-region MFDs system can be described by the following first order difference equations

$$n_{ii}(k_\mathrm{m}+1) = n_{ii}(k_\mathrm{m}) + T_\mathrm{m}\left(q_{ii}(k_\mathrm{m}) - M_{ii}(k_\mathrm{m}) - \sum_{h\in\mathcal{N}_i} M_{ii}^h(k_\mathrm{m}) + \sum_{h\in\mathcal{N}_i} M_{hi}^i(k_\mathrm{m})\right) \tag{1}$$

$$n_{ij}(k_\mathrm{m}+1) = n_{ij}(k_\mathrm{m}) + T_\mathrm{m}\left(q_{ij}(k_\mathrm{m}) - \sum_{h\in\mathcal{N}_i} M_{ij}^h(k_\mathrm{m}) + \sum_{h\in\mathcal{N}_i} M_{hj}^i(k_\mathrm{m})\right) \qquad i \neq j \tag{2}$$

where $k_\mathrm{m} = 0, 1, \ldots, K_\mathrm{m} - 1$ is the discrete time index, T_m [sec] the sample time period of the model (i.e. $t = k_\mathrm{m}T$) and $n_i(k_\mathrm{m}) = \sum_{j\in\mathcal{N}} n_{ij}(k_\mathrm{m})$ the total accumulation of region i. The exogenous variables $q_{ij}(k_\mathrm{m})$ [veh/sec] denote the (uncontrollable) traffic flow demand that is generated in region i at time step k_m with final destination in region j (i.e. $q_{ii}(k_\mathrm{m})$ is the demand generated in region i that has final destination in region i, without going through another region). The variables $M_{ij}^h(k_\mathrm{m})$ [veh/sec] denote the transfer flows from region i to region h that have final destination region j, while $M_{ii}(k_\mathrm{m})$ [veh/sec] is the internal trip completion rate in i with destination i.

We assume that for each region i there exists a production MFD between accumulation $n_i(k_\mathrm{m})$ and total production $P_i(n_i(k_\mathrm{m}))$ [veh.m/sec], which describes the performance of the system in an aggregated way. This MFD can be easily estimated using measurements from loop detectors and/or GPS trajectories. Transfer flows and internal trip completion rates are estimated corresponding to the production MFD of the region and proportionally to the accumulations

Figure 1: A network modeled as a multi-region MFDs system.

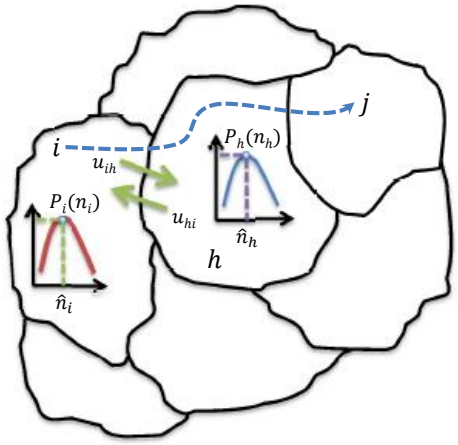

$n_{ij}(k_\mathrm{m})$ as follows

$$M_{ii}(k_\mathrm{m}) = \frac{n_{ii}(k_\mathrm{m})}{n_i(k_\mathrm{m})} \frac{P_i(n_i(k_\mathrm{m}))}{L_i} \tag{3}$$

$$M_{ij}^h(k_\mathrm{m}) = min\left\{ C_{hj}^i(n_h(k_\mathrm{m})), u_{ih}(k_\mathrm{m}) \frac{n_{ij}(k_\mathrm{m})}{n_i(k_\mathrm{m})} \frac{P_i(n_i(k_\mathrm{m}))}{L_i} \right\} \tag{4}$$

where L_i is the average trip length for region i, which is assumed to be independent of time and destination, internal or external, in i. The transfer flows $M_{ij}^h(k_\mathrm{m})$ are the minimum between the sending flow from region i (which only depends on the accumulations of the region), and the receiving capacity $C_{hj}^i(n_h(k_\mathrm{m}))$ [veh/sec] of region h. This flow capacity is a function of the accumulation $n_h(k_\mathrm{m})$ and is introduced to prevent overflow phenomena within the regions, i.e. each region i has a maximum accumulation $n_{i,\max}$

$$0 \leq n_i(k_\mathrm{m}) \leq n_{i,\max}, \forall i \in \mathcal{N} \tag{5}$$

If $n_i(k_\mathrm{m}) = n_{i,\max}$ the region reaches gridlock and all the inflows along the periphery are restricted. Finally, the control variables $u_{ih}(k_\mathrm{m}), \forall i \in \mathcal{N}, h \in \mathcal{N}_i$ denote the fraction of the flow that is allowed to transfer from region i to region h at time k_m. The values of the control variables are constrained by physical or operational constraints as follows

$$0 \leq u_{ih,\min} \leq u_{ih}(k_\mathrm{m}) \leq u_{ih,\max} \leq 1, \quad \forall i \in \mathcal{N}, h \in \mathcal{N}_i \tag{6}$$

where $u_{ih,\min}$, $u_{ih,\max}$ are the minimum and maximum permissible transferring rates of flows, respectively. Equations (1)–(4) are a discretized version of equations presented in Yildirimoglu *et al.* (2015) and represent the traffic dynamics in an N-region urban network considering the

heterogeneity effect and integrating an aggregated route choice model. Note, that these equations assume that drivers can choose any arbitrary sequence of regions as their path and cross region boundaries multiple times.

3 Feedback control structure

The nonlinear N-region MFDs system that was described in the previous section can be controlled in real-time by defining the values of the control variables $u_{ih}(k_\mathrm{m}), \forall i \in \mathcal{N}, h \in \mathcal{N}_i$. The control goal is to keep the traffic state of each region around a set value, so that the throughput is maximized and the region does not enter the saturated regime of the MFD. In this work, the following classical multivariable proportional-integral-type (PI) state feedback regulator is applied

$$\mathbf{u}(k_\mathrm{c}) = \mathbf{u}(k_\mathrm{c} - 1) - \mathbf{K}_\mathrm{P}\left[\mathbf{n}(k_\mathrm{c}) - \mathbf{n}(k_\mathrm{c} - 1)\right] - \mathbf{K}_\mathrm{I}\left[\mathbf{n}(k_\mathrm{c}) - \hat{\mathbf{n}}\right] \tag{7}$$

where k_c is the control discrete time index, $\mathbf{u}(k_\mathrm{c})$ is the control vector of $u_{ih}(k_\mathrm{c}), \forall i \in \mathcal{N}, h \in \mathcal{N}_i$, $\mathbf{n}(k_\mathrm{c}) \in \mathbb{R}^N$ the state vector of region accumulations $n_i(k_\mathrm{c}), \forall i \in \mathcal{N}$, $\hat{\mathbf{n}} \in \mathbb{R}^N$ the vector of the set points $\hat{n}_i$ for each region i and $\mathbf{K}_\mathrm{P}, \mathbf{K}_\mathrm{I} \in \mathbb{R}^{M \times N}$ are the proportional and integral gains, respectively. It should be noted that the number of control variables M depends on the network partition and the sets $\mathcal{N}_i, i \in \mathcal{N}$; however it is always greater than the number of state variables N for any network partition, since each region $i \in \mathcal{N}$ is equipped with (at least) one boundary controller $u_{ih}, h \in \mathcal{N}_i$ (the only case where $M = N$ is for $N = 2$, i.e. we only have two regions). Note also, that the states of the system consist of the aggregated accumulations $n_i, i \in \mathcal{N}$ and not all the accumulations n_{ij} described in equations (1)–(4). Finally, it should be emphasized that a well-known property of the PI regulator (7) is that it provides zero steady-state error (due to the existence of the integral term), i.e. $\mathbf{n}(k_\mathrm{c}) = \hat{\mathbf{n}}$ under stationary conditions.

The structure of the controller (7) is similar to the one used in Aboudolas and Geroliminis (2013); however here there are no control variables at the borders of the network but only at the borders between regions. As a consequence, there are no vehicles kept outside of the network in order to protect the congestion of the regions (which is also the case in Keyvan-Ekbatani *et al.* (2012)) and all the (gating) queues created by the controllers are internal to the network and thus affecting other movements. Moreover, in Aboudolas and Geroliminis (2013) the gain matrices $\mathbf{K}_\mathrm{P}, \mathbf{K}_\mathrm{I}$ are computed by applying linear control theory and solving the Riccati equation of a linearized version of the original nonlinear system. Here, the gain matrices as well as the vector of the set points of the controller $\hat{\mathbf{n}}$ are optimized in real-time by the use of an adaptive algorithm and based on real performance measurements. The closed-loop adaptive optimization scheme

that constantly updates the parameters of the controller is presented in the next section.

The state feedback regulator (7) is activated in real-time at each control interval T_c [sec] and only within specific time windows based on the current accumulations $\mathbf{n}(k_c)$ (i.e. by use of two thresholds $n_{i,\text{start}}$ and $n_{i,\text{stop}}$ and real-time measurements). The required real-time information of the vehicle accumulations $\mathbf{n}(k_c)$ can be directly estimated via loop detector time-occupancy measurements. Equation (7) calculates the fraction of flows $\mathbf{u}(k_c)$ to be allowed to transfer between neighborhood regions. In case the ordered values $u_{ih}(k_c)$ violate the constraints (6) they should be adjusted to become feasible, i.e. truncated to $[u_{ih,\min}, u_{ih,\max}]$. Moreover, the values of $\mathbf{u}(k_c - 1)$ used on the right-hand side of (7), should be the bounded values of the previous time step (i.e. after the application of the constraints) in order to avoid possible wind-up phenomena in the PI regulator. The obtained $u_{ih}(k_c)$ values are then used to derive the green time duration for the stages of the signalized intersections located at the boundaries of neighborhood regions. The ordered transferring flows are equally distributed to the corresponding intersections and converted to a transfer link green stage duration, with respect to the saturation flow of the link and the cycle time of the intersections. Note, that each controlled intersection can operate in a different cycle time, which means that the control decisions may be applied at different times in different locations, i.e. at the end of each intersection control cycle.

4 Adaptive optimization algorithm description

The parameters $\mathbf{K}_P$, $\mathbf{K}_I$, $\hat{\mathbf{n}}$ of the regulator (7) are updated in real-time based on measurements of an objective function, so as to optimize the performance of the controller. The Adaptive Fine-Tuning (AFT) algorithm is used for that purpose. AFT is a recently developed algorithm (see Kosmatopoulos and Kouvelas (2009), Kouvelas *et al.* (2011a) for details) for tuning the parameters (in the specific case the gain matrices and set points) of controllers in an optimal way. It is an iterative algorithm that is based on machine learning techniques and adaptive optimization principles and adjusts the control gains and set points to the variations of the process under control. The working principle of the integrated closed-loop system (PI regulator and AFT) is presented in Figure 2 and may be summarized as follows:

- The N-region MFDs system is controlled in real-time by the PI regulator (7) which includes a number of tunable parameters $\boldsymbol{\theta} = \text{vec}\,(\mathbf{K}_P, \mathbf{K}_I, \hat{\mathbf{n}}) \in \mathbb{R}^{2\times(M\times N)+N}$.
- At the end of appropriately defined periods T_o (e.g. at the end of each day), AFT algorithm receives the value of the real (measured) performance index J (e.g. total delay of the system), as well as the values of the most significant measurable external disturbances $\mathbf{x}$ (e.g. aggregated demand). Note that the scalar performance index $J\,(\boldsymbol{\theta}, \mathbf{x})$ is a (generally

Figure 2: The integrated closed-loop adaptive system (PI regulator and AFT algorithm).

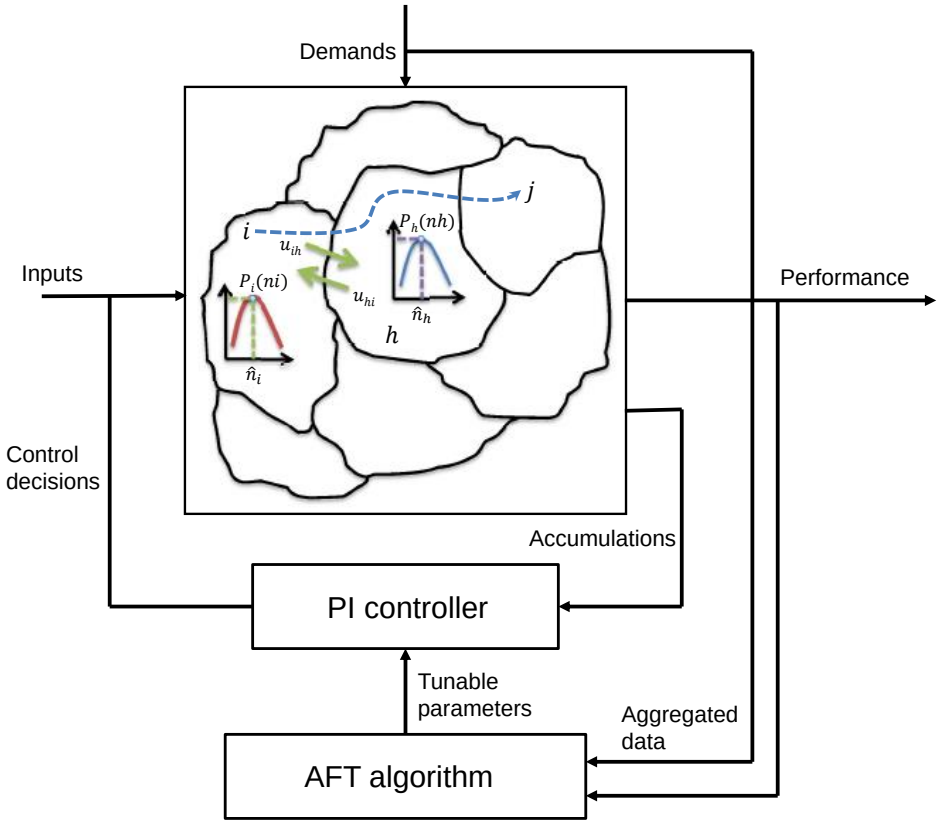

unknown) function of the external factors $\mathbf{x}$ and the tunable parameters $\boldsymbol{\theta}$.

- Using the measured quantities (the samples of which increase iteration by iteration), AFT calculates new tunable parameter values to be applied at the next period (e.g. the next day) in an attempt to improve the system performance.
- This (iterative) procedure is continued over many periods (e.g. days) until the algorithm converges and an optimal performance is reached; then, AFT algorithm may remain active for continuous adaptation or can be switched off and re-activated at a later stage.

The main component of the employed algorithm is a universal approximator $\hat{J}(\boldsymbol{\theta}, \mathbf{x})$ (e.g., a polynomial-like approximator or a neural network) that is used in order to obtain an approximation of the nonlinear mapping $J(\boldsymbol{\theta}, \mathbf{x})$, based on all previous samples. At each algorithm iteration k_o, the following main steps are taking place (the reader is referred to Kosmatopoulos and Kouvelas (2009), Kouvelas *et al.* (2011a) for a complete description of the algorithm):

1. A new polynomial approximator with L_g regressor terms is produced, which has the following structure

$$\hat{J}^{(k_o)}(\boldsymbol{\theta}, \mathbf{x}) = \boldsymbol{\vartheta}^{\top}(k_o)\boldsymbol{\phi}^{(k_o)}(\boldsymbol{\theta}, \mathbf{x}) \tag{8}$$

where $L_{\mathrm{g}} = \min\left\{2\left(k_{\mathrm{o}}-1\right), L_{\mathrm{g,max}}\right\}$ (i.e. the number increases with iterations up to a maximum value), $\boldsymbol{\vartheta}(k_{\mathrm{o}}) \in \mathbb{R}^{L_{\mathrm{g}}}$ are the weights of the approximator for iteration k_{o} (equivalent to the synaptic connections in neural networks) and $\boldsymbol{\phi}^{(k_{\mathrm{o}})}(\boldsymbol{\theta}, \mathbf{x})$ is a vector with L_{g} sigmoidal functions of polynomials constructed using the elements of vectors $\boldsymbol{\theta}, \mathbf{x}$ (nonlinear activation functions or neurons).

2. The values of the weights $\boldsymbol{\vartheta}(k_{\mathrm{o}})$ are obtained by the solution of the following optimization problem

$$\boldsymbol{\vartheta}(k_{\mathrm{o}}) = \arg\min_{\boldsymbol{\vartheta}(k_{\mathrm{o}})} \frac{1}{2}\sum_{\ell=1}^{k_{\mathrm{o}}}\left(J_{\ell} - \boldsymbol{\vartheta}(k_{\mathrm{o}})^{\intercal}\boldsymbol{\phi}_{\ell}^{(k_{\mathrm{o}})}\right)^{2} \tag{9}$$

3. Many randomly chosen candidate perturbations $\Delta\boldsymbol{\theta}^{(p)}(k_{\mathrm{o}})$, $p \in \{1, 2, \ldots, K\}$ are generated. The effect of all candidate new vectors $\boldsymbol{\theta}^{(p)}(k_{\mathrm{o}}+1) = \boldsymbol{\theta}^{*}(k_{\mathrm{o}}) + \Delta\boldsymbol{\theta}^{(p)}(k_{\mathrm{o}})$ (where $\boldsymbol{\theta}^{*}(k_{\mathrm{o}})$ is the "best" set of tunable parameters until the k_{o}-th experiment, i.e. the one with the best performance so far), as well as $\boldsymbol{\theta}^{(-p)}(k_{\mathrm{o}}+1) = \boldsymbol{\theta}^{*}(k_{\mathrm{o}}) - \Delta\boldsymbol{\theta}^{(p)}(k_{\mathrm{o}})$ to the system performance is estimated by using the approximator mentioned above, i.e.

$$\hat{J}\left(\boldsymbol{\theta}^{(\pm p)}(k_{\mathrm{o}}+1), \hat{\mathbf{x}}(k_{\mathrm{o}}+1)\right) = \boldsymbol{\vartheta}(k_{\mathrm{o}})^{\intercal}\boldsymbol{\phi}^{(k_{\mathrm{o}})}\left(\boldsymbol{\theta}^{(\pm p)}(k_{\mathrm{o}}+1), \hat{\mathbf{x}}(k_{\mathrm{o}}+1)\right) \tag{10}$$

where $\hat{\mathbf{x}}(k_{\mathrm{o}}+1)$ is an estimate of the external disturbances $\mathbf{x}$ for the next experiment $k_{\mathrm{o}}+1$.

4. The vector $\boldsymbol{\theta}(k_{\mathrm{o}}+1)$ that corresponds to the best estimate, i.e.

$$\boldsymbol{\theta}(k_{\mathrm{o}}+1) = \arg\min_{\boldsymbol{\theta}^{(\pm p)}(k_{\mathrm{o}}+1)} \hat{J}\left(\boldsymbol{\theta}^{(\pm p)}(k_{\mathrm{o}}+1), \hat{\mathbf{x}}(k_{\mathrm{o}}+1)\right) \tag{11}$$

is selected to determine the new values for the tunable parameters $\boldsymbol{\theta}(k_{\mathrm{o}}+1)$ to be applied at the next period $k_{\mathrm{o}}+1$ (e.g. the next day).

By the application of steps 1–4 described above AFT changes the parameters of the PI regulator at each iteration. Although feedback regulators are found to be quite robust to moderate parameter value changes, it should be noted that these changes should be within certain limits in order to avoid stability issues. To this end, some user-defined permissible bounds are introduced in AFT for all parameters $\boldsymbol{\theta}$, i.e.

$$\boldsymbol{\theta}_{\min} \leq \boldsymbol{\theta}(k_{\mathrm{o}}) \leq \boldsymbol{\theta}_{\max} \tag{12}$$

This means that all the candidate vectors $\boldsymbol{\theta}(k_{\mathrm{o}}+1)$ generated in step 2 above are first projected to the permissible domain $\boldsymbol{\Theta} = [\boldsymbol{\theta}_{\min}, \boldsymbol{\theta}_{\max}]$ and then applied to the approximator for evaluation. The domain $\boldsymbol{\Theta}$ is crucial for the safe and efficient performance of the algorithm and can be in some cases defined by applying stability conditions to the system under control.

5 Network description and simulation set-up

The efficiency of the adaptive system described in the previous sections is tested in microsimulation experiments. The urban network of Barcelona, Spain is used as the test site, which is modeled and calibrated via the AIMSUN microscopic environment (Figure 3(a)). The network covers an area of 15 square kilometers with about 600 intersections and 1500 links of various lengths. The number of lanes for through traffic varies from 2 to 5 and the free flow speed is 45 kilometers per hour. Traffic lights at signalized intersections are operating on multi-phase fixed-time plans with constant (but not equal) cycle lengths. For the simulation experiments, typical loop-detectors have been installed around the middle of each network link. The OD-based demand used for the simulations provides a good replication of real life conditions as it generates realistic traffic congestion patterns in the network. The duration of the simulation is 2 hours including a 15 minutes warm-up period. In the no control case (where the real fixed-time plans are applied to the intersections) the network faces some serious congestion problems, with queues spilling back to upstream intersections. Note, that the Dynamic Traffic Assignment (DTA) module of the simulator (C-Logit route choice model) is activated every 3 minutes, therefore the drivers adapt to the traffic conditions.

As in most cities of the world, traffic congestion in the city of Barcelona is unevenly distributed, creating multiple pockets of congestion in different areas of the network. As MFD depends on the distribution of link densities (occupancies, speeds), partitioning heterogeneously loaded cities with uneven distribution of congestion into homogeneous regions is a possible solution to take advantage of well-defined MFDs. In fact, the outflow of the network is a function of both average and variance of link densities. Since traffic conditions are spatially correlated in adjacent roads and congestion propagates from adjacent links, describing the main pockets of congestion in a city with a small number of clusters without the need for detailed information in every link of the network is conceivable. By partitioning, we aim to group spatially-connected links with close density values within a cluster, which increases the network flow for the same average density. Spatial connectivity is a necessary condition that makes feasible the application of perimeter control strategies. The partitioning algorithm used in this study is an optimization framework called "Snake" which considers heterogeneity index as a main objective function and contiguity is forced explicitly by imposing constraints (Saeedmanesh and Geroliminis, 2015). This approach needs desired number of clusters as a predefined input and it obtains optimal number of clusters by evaluating heterogeneity metric for different number of clusters. By use of this algorithm, the network of Barcelona is partitioned into 4 homogeneous regions that are shown in Figure 3(b).

This partitioning derives $M = 6$ control variables (i.e. $u_{14}, u_{24}, u_{34}, u_{41}, u_{42}, u_{43}$) and $N = 4$

Figure 3: The test site of Barcelona, Spain: (a) simulation model with four regions; (b) results of the clustering algorithm and controlled intersections. Blue circles correspond to intersections belonging to u_{14}, red to u_{24}, green to u_{34} and black to u_{4h}, $h = 1, 2, 3$.

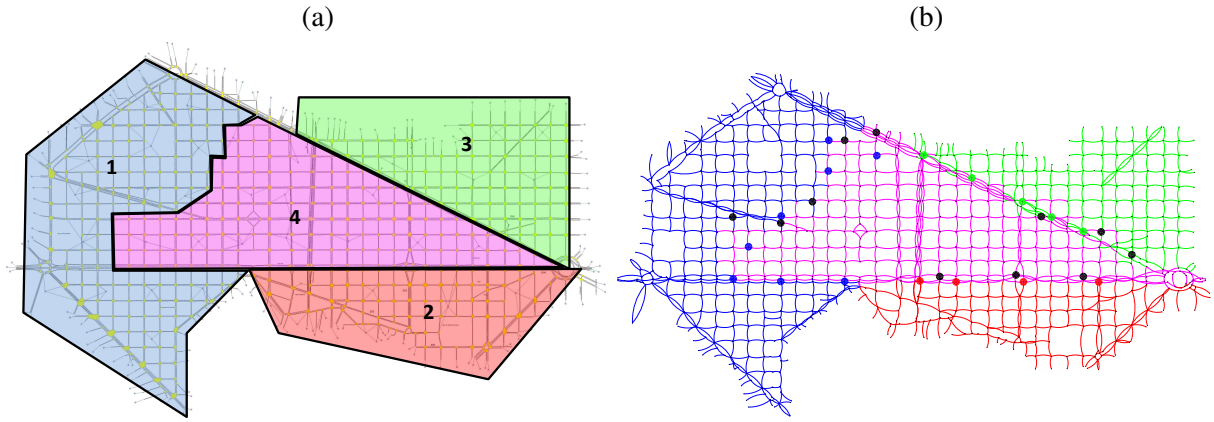

state variables (n_1, n_2, n_3, n_4). The PI regulator is applied every $T_c = 90$sec and the control decisions (after modified to satisfy the operational constraints) are forwarded for application to 28 signalized intersections which are all across the boundaries of region 4. As shown in Figure 3(b), there are 8 intersections for applying u_{14} (blue circles), 4 for u_{24} (red circles), 5 for u_{34} (green circles), 5 for u_{41}, 3 for u_{42} and 3 for u_{43}. All the intersections that control the outflow of region 4 are indicated in Figure 3(b) with black circles although they correspond to different control variables. Their location at the borders of region 4 in Figure 3(b) indicates the control variable in which they belong.

6 Simulation results

This section presents the results obtained by the simulation experiments. AFT is run for 100 iterations starting from an initial point where $\mathbf{K}_P = \mathbf{K}_I = \mathbf{0}^{M\times N}$. For these values the regulator (7) operates as a fixed-time policy and this point is equivalent to the no control (NC) case (i.e. the actual fixed-time plans of the city are applied). The initial values for the set points $\hat{\mathbf{n}}$ are obtained from the MFDs of the NC case and are equal to $\hat{\mathbf{n}} = [1700, 600, 600, 2400]^T$. The performance index of AFT (i.e. the objective function J that tries to minimize) is selected to be the total delay of the system, which is available after the end of the simulation. In each iteration the whole simulation of 2 hours is run with the same parameters for the controller. At the end of the simulation AFT is called to calculate the new values of $\mathbf{K}_P, \mathbf{K}_I, \hat{\mathbf{n}}$ to be used in the next iteration.

Figure 4: (a) Evolution of total network delay and (b) total network throughput for the 100 iterations of AFT.

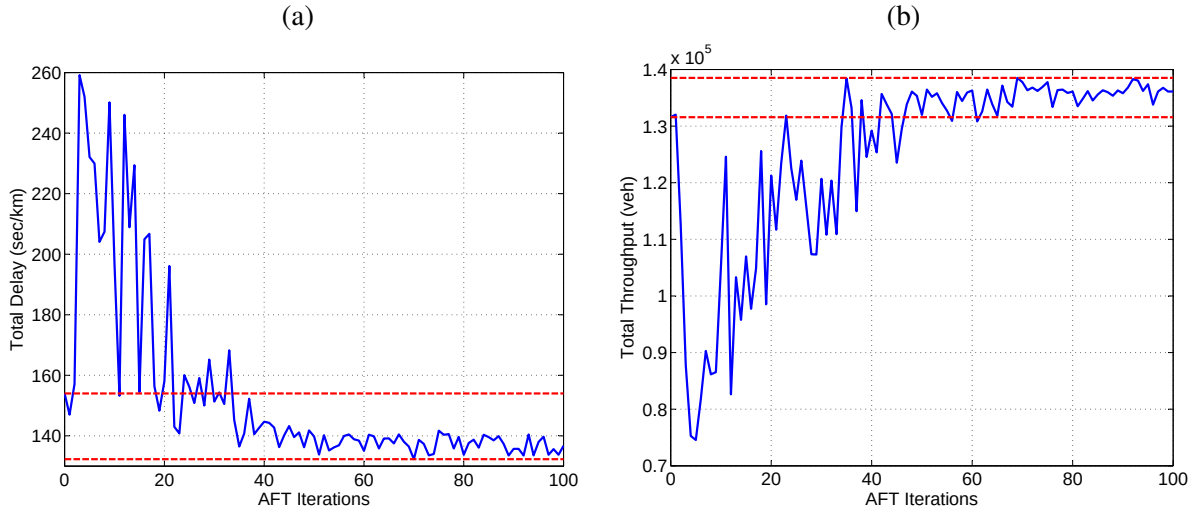

Figure 4(a) presents the evolution of the total delay (measured in sec/km) over the iterations of the algorithm. The starting point (NC) as well as the best controller (BC) obtained through the process are illustrated with red dashed lines. For the first iterations of the algorithm the value of the total delay is very high, since there are not many samples and the approximator cannot learn from the previous experiments. As the number of iterations increases the learning process becomes better and the objective function exhibits a convergent behavior. Figure 4(b) presents the total throughput of the network (total number of vehicles exiting the network) for the same simulations. Although it is not taken into account by AFT it provides another index of the tuning performance. It can be seen that the total throughput of the network has the reverse behavior of the total delay (i.e. simulations with higher throughput have lower delays); however by carefully inspecting the simulation results this relation is not always consistent.

Figure 5(a) illustrates the control decisions $\mathbf{u} = [u_{14}, u_{24}, u_{34}, u_{41}, u_{42}, u_{43}]^\intercal$ for every k_c, for the simulation with the best results in terms of total delay (BC). The controller is activated at $k_c = 24$ and stays active until the end of the simulation, as the accumulations are continuously increasing. Figure 5(b) shows the production MFD for the whole network (total production over total accumulation) for the no control case and the best controller obtained after the 100 iterations. The production reduces to less than 2000 km.veh/control cycle for the no control case (congested regime of the MFD), while for the BC case it is always higher than 2500 km.veh/control cycle (the control cycle T_c is equal to 90 seconds). Figure 6(a) and (b) present the time series of the network accumulation and production, respectively, for the same cases.

Table 1 displays the evaluation criteria for simulations NC and BC. It can be seen that the

Figure 5: (a) Control decisions over simulation time for the BC case; (b) production MFD for the whole network.

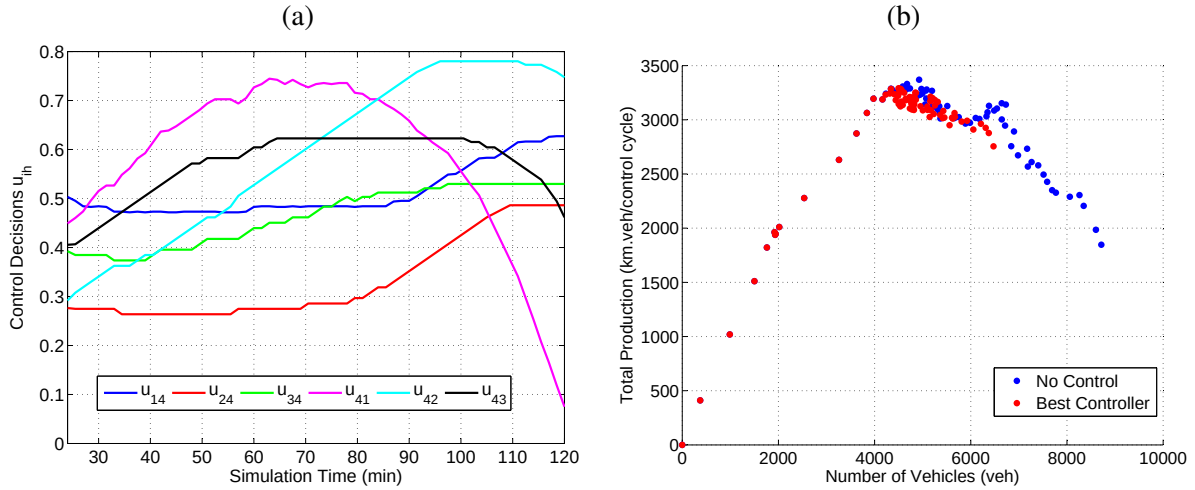

Figure 6: Time series of network (a) accumulation and (b) production for no control and best controller.

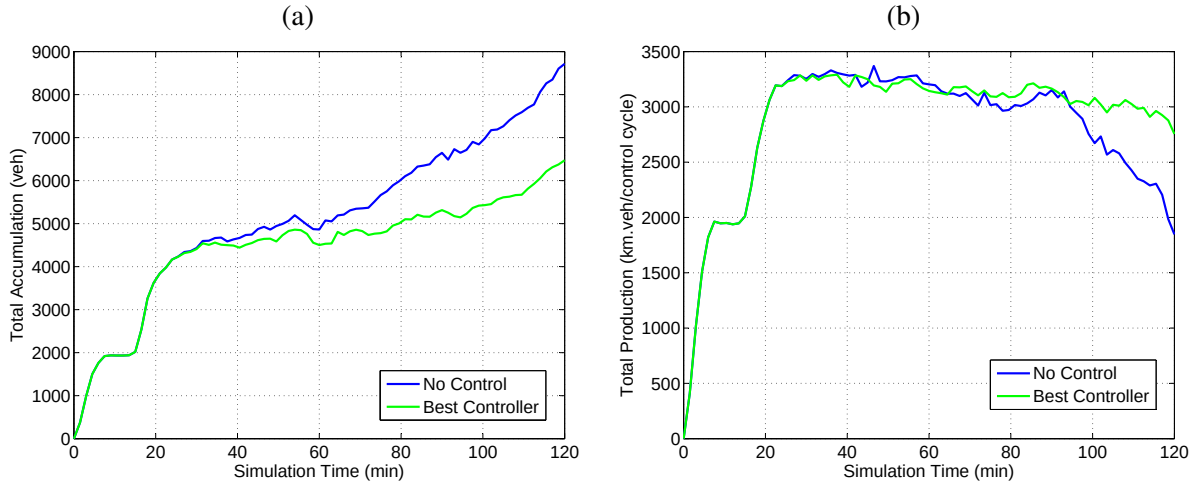

controller obtained from AFT improves the no control case for all the metrics. More specifically, we obtain an improvement of some 14% for the total delay and about 11% for the average speed. Moreover, BC controller manages to serve more vehicles during the 2 hours as the total input and total output are higher. There are less virtual queues in the network and at the end of the simulation there are less vehicles inside the network (as the NC case faces gridlock phenomena) and less vehicles waiting to enter. The percentage of improvement of BC over NC for all criteria can be seen in the third column of Table 1.

Table 1: Evaluation criteria for NC and BC simulations.

Evaluation criteria	BC	NC	Difference (%)	Units
Total Delay	132.29	154.01	-14.10	sec/km
Space-mean Speed	18.26	16.46	10.94	km/h
Total Input	148619	147087	1.04	veh
Max Virtual Queue	6608	8126	-18.68	veh
Mean Queue	3397.36	4729.98	-28.17	veh
Stop Time	93.82	112.85	-16.86	sec/km
Total Travel Time	11704.21	12297.68	-4.83	h
Total Travelled Distance	223222.64	211871.63	5.36	km
Travel Time	197.12	218.75	-9.89	sec/km
Vehicles Inside	10851	15514	-30.06	veh
Vehicles Outside	137768	131573	4.71	veh
Vehicles Waiting to Enter	6595	8126	-18.84	veh

Figure 7(a) and (b) show the production MFDs of all regions for NC and BC respectively. For the BC case, the conditions in regions 1, 3 and 4 are improved as they only have a few states in the congested regime, whereas region 2 remains uncongested in both cases. The improvement for the three regions that face congestion problems at the NC case can be also seen in Figure 8(a) and (b) that present the time series of productions and accumulations over the simulation time for all regions. At the last 30 minutes of the simulation the productions of regions 1, 3 and 4 are kept high in the BC case, as opposed to NC that are reduced because of congestion. The superiority of BC can be also seen at the accumulations of these three regions at the end of the simulation.

7 Conclusions and future work

The efficiency of an adaptive optimization algorithm applied to a PI feedback regulator was tested in microsimulation. The simulation results indicate that the integrated control scheme can improve the network performance compared to fixed-time signal plans. AFT algorithm tunes the parameters of the multivariable controller (gain matrices and set points) iteration by iteration, so as to achieve a desirable performance. One disadvantage of the algorithm is that it has a "spiky" behavior during the first iterations (e.g. days) of application. This is because of the low number of available measurements (samples) that make the learning process difficult. This behavior makes the online applicability of the algorithm cumbersome, as it can lead to system

Figure 7: Production MFDs for the four regions for (a) NC and (b) BC simulations.

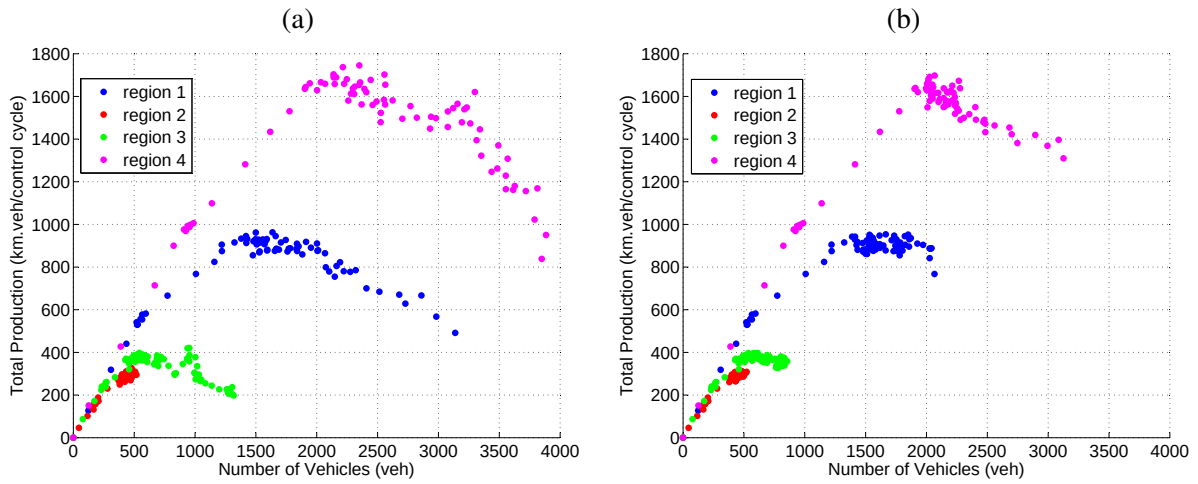

Figure 8: Time series of (a) accumulations and (b) productions for the four regions (solid lines represent NC and dashed lines BC).

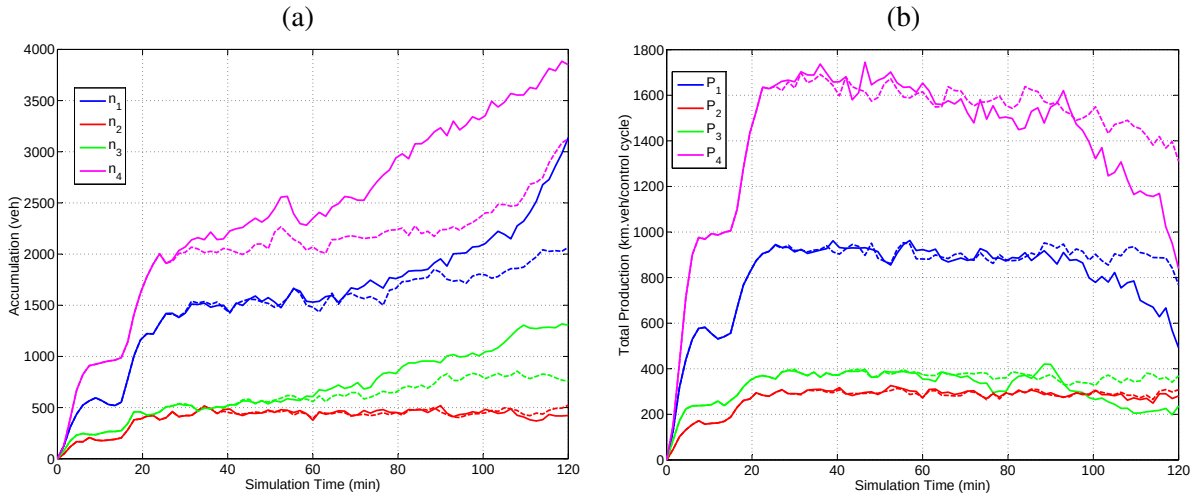

performance that is too far from optimal and create undesirable situations. To overcome this difficulty, future work will deal with application of AFT algorithm to the macroscopic model presented in Section 2 (equations (1)–(4)) instead of applying it directly to the controlled process. In this case, a model-based optimization procedure will be employed to the overall scheme and after the convergence of the algorithm the obtained best controller can be applied to the real system (plant). The MFD model provides a replication of the plant and AFT can optimize the performance of the PI controller based on many runs with the model (until it converges) before applying one iteration to the plant. The whole procedure can be integrated online as the running time of AFT and the system dynamics is negligible.

8 References

Aboudolas, K. and N. Geroliminis (2013) Perimeter and boundary flow control in multi-reservoir heterogeneous networks, *Transportation Research Part B: Methodological*, **55**, 265–281.

Aboudolas, K., M. Papageorgiou, A. Kouvelas and E. Kosmatopoulos (2010) A rolling-horizon quadratic-programming approach to the signal control problem in large-scale congested urban road networks, *Transportation Research Part C: Emerging Technologies*, **18** (5) 680–694.

Ampountolas, K. and A. Kouvelas (2015) Real-time estimation of critical values of the macroscopic fundamental diagram for maximum network throughput, paper presented at the *Transportation Research Board 94th Annual Meeting*, no. 15-1779.

Daganzo, C. F. (2007) Urban gridlock: macroscopic modeling and mitigation approaches, *Transportation Research Part B: Methodological*, **41** (1) 49–62.

Diakaki, C., V. Dinopoulou, K. Aboudolas, M. Papageorgiou, E. Ben-Shabat, E. Seider and A. Leibov (2003) Extensions and new applications of the traffic-responsive urban control strategy: Coordinated signal control for urban networks, *Transportation Research Record: Journal of the Transportation Research Board*, **1856** (1) 202–211.

Diakaki, C., M. Papageorgiou and K. Aboudolas (2002) A multivariable regulator approach to traffic-responsive network-wide signal control, *Control Engineering Practice*, **10** (2) 183–195.

Farges, J., J. Henry and J. Tufal (1983) The PRODYN real-time traffic algorithm, paper presented at the *Proc. 4th IFAC Symposium on Trasportation Systems*, 307–312, Baden-Baden, Germany.

Gartner, N. (1983) OPAC: A demand-responsive strategy for traffic signal control, *Transportation Research Record: Journal of the Transportation Research Board*, (906) 75–84.

Geroliminis, N. and C. F. Daganzo (2008) Existence of urban-scale macroscopic fundamental diagrams: Some experimental findings, *Transportation Research Part B: Methodological*, **42** (9) 759–770.

Geroliminis, N., J. Haddad and M. Ramezani (2013) Optimal perimeter control for two urban regions with macroscopic fundamental diagrams: A model predictive approach, *IEEE Transactions on Intelligent Transportation Systems*, **14** (1) 348–359.

Godfrey, J. W. (1969) The mechanism of a road network, *Traffic Engineering & Control*, **11** (7) 323–327.

Haddad, J. and N. Geroliminis (2012) On the stability of traffic perimeter control in two-region urban cities, *Transportation Research Part B: Methodological*, **46** (9) 1159–1176.

Haddad, J. and B. Mirkin (2015) Distributed adaptive MFD-based control for large-scale urban road networks, paper presented at the *Transportation Research Board 94th Annual Meeting*, no. 15-1735.

Hunt, P., D. Robertson, R. Bretherton and M. C. Royle (1982) The SCOOT on-line traffic signal optimisation technique, *Traffic Engineering & Control*, **23** (4).

Ji, Y. and N. Geroliminis (2012) On the spatial partitioning of urban transportation networks, *Transportation Research Part B: Methodological*, **46** (10) 1639–1656.

Keyvan-Ekbatani, M., A. Kouvelas, I. Papamichail and M. Papageorgiou (2012) Exploiting the fundamental diagram of urban networks for feedback-based gating, *Transportation Research Part B: Methodological*, **46** (10) 1393–1403.

Kosmatopoulos, E. B. and A. Kouvelas (2009) Large scale nonlinear control system fine-tuning through learning, *IEEE Transactions on Neural Networks*, **20** (6) 1009–1023.

Kouvelas, A., K. Aboudolas, E. B. Kosmatopoulos and M. Papageorgiou (2011a) Adaptive performance optimization for large-scale traffic control systems, *IEEE Transactions on Intelligent Transportation Systems*, **12** (4) 1434–1445.

Kouvelas, A., K. Aboudolas, M. Papageorgiou and E. B. Kosmatopoulos (2011b) A hybrid strategy for real-time traffic signal control of urban road networks, *IEEE Transactions on Intelligent Transportation Systems*, **12** (3) 884–894.

Lowrie, P. (1982) SCATS: The Sydney co-ordinated adaptive traffic system – Principles, methodology, algorithms, paper presented at the *Proc. IEE International Conference on Road Traffic Signalling*, 67–70, London, England.

Mirchandani, P. and L. Head (1998) RHODES – A real-time traffic signal control system: Architecture, algorithms, and analysis, paper presented at the *TRISTAN III*, vol. 2, San Juan, Puerto Rico.

Papageorgiou, M., C. Diakaki, V. Dinopoulou, A. Kotsialos and Y. Wang (2003) Review of road traffic control strategies, *Proceedings of the IEEE*, **91** (12) 2043–2067.

Saeedmanesh, M. and N. Geroliminis (2015) Clustering of heterogeneous networks with directional flows based on "snake" similarities, paper presented at the *Transportation Research Board 94th Annual Meeting*, no. 15-1354.

Yildirimoglu, M., M. Ramezani and N. Geroliminis (2015) A rolling horizon approach for route guidance in large-scale networks, paper presented at the *Transportation Research Board 94th Annual Meeting*, no. 15-2073.